Original Article
Special Topic: Advances in Bladder Cancer Research
Current Urology
OPEN

Preliminary study of the mechanism of isolinderalactone inhibiting the malignant behavior of bladder cancer

Qun Wang[a], Wenkai Xu[b], Lu Ying[c,d], Hongjin Shi[a], Yuxin Sun[a], Wei Feng[a], Haole Xu[a], Jun Xie[a], Hairong Wei[a], Zhao Yang[c,d,*], Haifeng Wang[a,*]

[a]Department of Urology, The Second Affiliated Hospital of Kunming Medical University, Kunming, China; [b]Department of Urology, The Second People's Hospital of Xindu District, Chengdu, China; [c]College of Life Science and Technology, Innovation Center of Molecular Diagnostics, Beijing University of Chemical Technology, Beijing, China; [d]College of Life Science and Technology, Key Laboratory of Protection and Utilization of Biological Resources in Tarim Basin of Xinjiang Production and Construction Corps, Tarim University, Alar, Xinjiang, China

Abstract

Background: Isolinderalactone (ILL), extracted from the dried tubers of *Linderae aggregate,* has multiple functions, such as antioxidation, antitumor, and anti-infection effects. However, there have been few studies on ILL's antitumor role and no reports on its role in bladder cancer (BC).

Materials and methods: Human BC cell lines T24 and EJ-1 were treated with different concentrations of ILL (0, 10, 20, 50, 100, 200, 400, 600, 800, and 1000 μmol/L), and the cell proliferation inhibition rate was analyzed using the CCK-8 assay. The effect of ILL on T24 and EJ-1 cell cycle inhibition and apoptosis was examined using flow cytometry. Immunoblotting was used to detect the levels of apoptosis-related proteins, BAX, BAK1, and CYCS, in BC cells of the control and ILL-treated groups, and quantitative PCR experiments were performed to detect the apoptosis-related gene expression of *CASP10*, *CYCS*, *BAX*, *BCL-2*, *CASP8*, and *BAK1*. T24 and EJ-1 tumor-bearing mouse models were established and divided into vehicle control, low-dose (10 mg/kg) and high-dose (20 mg/kg) groups, with 5 mice in each group. Hematoxylin and eosin staining and immunohistochemistry were used to detect changes in apoptosis-related proteins in vivo.

Results: The CCK-8 assay showed that in vitro, ILL significantly inhibited the proliferation of the T24 and EJ-1 BC cell lines. Flow cytometry and immunoblotting results showed that ILL increased mitochondrial permeability by upregulating proapoptotic proteins BAK1 and BAX, promoting CYCS release and significantly inducing cell cycle arrest at G0/G1 phase. In vivo, on day 25 of administration, tumor inhibition rates in T24 and EJ-1 tumor-bearing mice were up to 75.24% and 47.43%, respectively, in the ILL high-dose–treated and 71.58% and 43.89%, respectively, in the ILL low-dose–treated groups.

Conclusions: Isolinderalactone controls BC progression by inducing apoptosis, suggesting that ILL may be an effective drug for the treatment of BC.

Keywords: Bladder cancer; Isolinderalactone; Mitochondrial apoptosis

1. Introduction

According to GLOBOCAN data, there will be approximately 570,000 new cases of bladder cancer (BC) and 210,000 BC-related deaths globally in 2020, posing a significant threat to human life and health.[1] Clinically, BC is classified into muscle-invasive BC (MIBC) and non–muscle-invasive BC (NMIBC), according to the degree of tumor infiltration. Currently, although patients with NMIBC can be treated through surgery, chemotherapy, or Bacillus Calmette-Guérin (BCG) treatment, 50% of the patients still experience relapse and 20% eventually progress to MIBC after systemic therapy.[2,3] In addition, even after receiving systemic chemotherapy or radical cystectomy, 50% of patients with MIBC continue to face challenges, such as systemic organ metastases from the lesion within 2 years of diagnosis and may even succumb to these complications.[4] For metastatic MIBC, cisplatin-based systemic chemotherapy is the first-line treatment, but the prognosis is unsatisfactory because of inherent or acquired cisplatin resistance and severe adverse reactions.[5] Moreover, long-term chemotherapy not only imposes physical and psychological burdens on patients but also places significant economic pressure on them because of the exorbitant costs associated with diagnosis and treatment. Therefore, exploring potential novel therapeutic agents against BC is currently a top priority in BC treatment.

Chinese herbal medicine is a treasure trove of treatments and interventions. The clinical applications of artemisinin for malaria

*Corresponding Authors: Haifeng Wang, Department of Urology, The Second Affiliated Hospital of Kunming Medical University, Yunnan Institute of Urology, Kunming, 650101, China. E-mail: wanghaifeng@kmmu.edu.cn (H. Wang); Zhao Yang, College of Life Science and Technology, Beijing University of Chemical Technology, Beijing, 100029, China. E-mail: yangzhao@mail.buct.edu.cn (Z. Yang).

Qun Wang, Wenkai Xu, and Lu Ying have contributed equally to this work.

Current Urology, (2025) 19, 1, 49–58

Received August 26, 2023; Accepted March 19, 2024.

http://dx.doi.org/10.1097/CU9.0000000000000259

and berberine for type 2 diabetes have aroused widespread interest in Chinese herbal medicine research.[6,7] Chinese herbal extracts were used to treat cancers because of their efficacy, safety, and accessibility.[8] In addition to the anticancer chemotherapeutic drug paclitaxel, Qici Sanling decoction[9] and Wogonin and its analogs[10] also demonstrated therapeutic potential for BC, but their specific mechanisms and clinical efficacies remain unclear. Therefore, the discovery of efficacious drugs with clear mechanisms to provide a certain foundation for adjuvant clinical treatment is warranted. Isolinderalactone (ILL) is extracted from dried tuber of Lauraceae family. In addition to its anti-inflammatory effects, it also has antitumor effects on various tumors. For example, ILL inhibited the invasion and migration of human lung cancer cells by downregulating the expression of matrix metalloproteinases.[11] Isolinderalactone induced apoptosis of breast cancer cells in vitro and in vivo by increasing the protein expression level of suppressor of cytokine signaling 3 while reducing the phosphorylation of signal transducer and activator of transcription 3.[12] In addition, ILL has antiproliferative effects against human glioblastomas.[13,14] However, whether ILL inhibits BC progression and its molecular mechanism of action in BC is unknown. Therefore, we investigated whether ILL inhibited BC growth in vitro and in vivo and the underlying mechanisms of this effect.

2. Materials and methods

2.1. Reagents and cell culture

The ILL monomer (purity >98%), a traditional Chinese medication, provided by Chengdu Desite Biotechnology Co., LTD (Chengdu, China), was dissolved into a storage solution containing 10 mM dimethyl sulfoxide (DMSO) (Solarbio, China) and stored at 4°C in the dark. Figure 1 shows the chemical structure of ILL. All other reagents were purchased from commercial sources. The human BC cell lines T24 and EJ-1 and the immortalized human normal bladder epithelial cell line SV-HUC-1 were obtained from the Beijing Beina Chuanglian Biotechnology Institute and cultured in RPMI-1640 medium (Hyclone, South Logan, UT, USA), 10% fetal bovine serum (FBS; Gibco, USA) supplemented with 100 U/mL penicillin, and 0.1 mg/mL streptomycin (Gibco, Grand Island, NY, USA) in an incubator at 37°C with 5% CO_2.

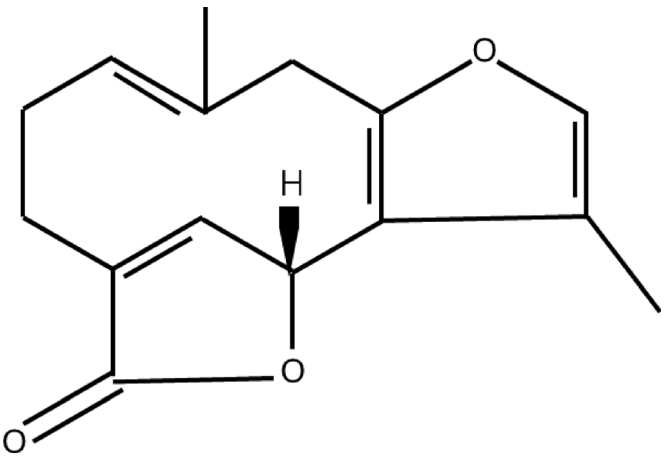

Figure 1. Structure of ILL+. ILL = isolinderalactone.

2.2. Cell growth inhibition assay

Normal urothelial (SV-HUC-1) and BC (T24 and EJ-1) cell lines were treated with ILL at 0, 10, 20, 50, 100, 200, 400, 600, 800, or 1000 μmol/L. The cells (20,000 cells/0.2 mL) were cultured in 96-well plates for 24 or 48 hours. When experimental termination was reached, 100 μL of a serum-free CCK8 (C0037; Beyotime, China) solution prepared in advance was added to each well and incubated for 2 hours in an incubator at 37°C. The absorbance was measured at 450 nm using a Multiskan FC microplate meter (51119080; Thermo Fisher Scientific, Waltham, MA, USA). The results were determined as cell viability where cell viability = [(As-Ab)/(Ac-Ab)] × 100%, in which As, Ac, and Ab are the absorbance measured in the experimental, control, and blank groups, respectively. The experimental results were statistically analyzed using GraphPad Prism statistical software (version 8.0) to calculate the IC_{50} values.

2.3. Wound healing assay

T24 and EJ-1 cells were seeded in 6-well plates at a density of 1×10^6 cells/well in 2 mL. When the cells were approximately 95% confluent, a vertical scratch was made with a 200-μL pipette tip, and the cells were washed 2 to 3 times with phosphate buffer saline (PBS) and then cultured in serum-free medium. The ImageJ software was used to assess the scratch area and determine the cell migration rate after cell images were collected under a microscope at 0, 12, 24, and 36 hours. Cell migration rate = (initial scratch area - scratch area at time t)/initial scratch area. The GraphPad Prism statistical software (version 8.0) was used for the data analysis.

2.4. Cell cycle assay

T24 and EJ-1 cells were inoculated at a density of 3×10^5 cells/well in 2 mL in 6-well plates. To synchronize the cell cycle after cell attachment, the medium was replaced with serum-free RPMI medium for 24 hours. In the control and experimental groups, 2 mL of 10% FBS complete medium and 10% FBS complete medium containing different concentrations of ILL (250 or 350 μmol/L) were added, respectively. After 48 hours, cells were harvested and fixed with 70% precooled ethanol at 4°C overnight. Cells were then washed using precooled PBS and cycling detection kit (Solarbio, Beijing, China), and were stained according to the manufacturer's instructions. After incubation at 37°C in the dark for 15 minutes, the cells were detected using flow cytometry. The FlowJo_V10 software was used to analyze the percentages of different cell cycles.

2.5. Cell apoptosis assay

T24 and EJ-1 cells were cultured in 6-well plates at a density of 3×10^5 cells/well in 2 mL. The experimental group was treated with 10% FBS complete medium containing different ILL concentrations (250 or 350 μmol/L) for 48 hours. After 48 hours, the cells were harvested and analyzed using an Annexin V-FITC apoptosis detection kit (Beyotime). The cells were incubated in the dark for 20 minutes, and flow cytometry was used to detect the distribution of apoptosis. The percentage of apoptotic cells was calculated using the FlowJo V10 software.

2.6. Quantitative real-time PCR

T24 and EJ-1 cells were divided into control and experimental groups, and both groups were treated with 300 μmol/L ILL for 48 hours. Total RNA was extracted with an RNA extraction kit (DP430; Tiangen, China), according to the manufacturer's instructions. The extracted RNA was then reverse transcribed into cDNA using a FastKing RT kit (KR116-02, Tiangen) and stored at –20°C for subsequent experiments. A QuantStudio1 real-time PCR

System (A40425, Thermo Fisher Scientific) and PowerUp SYBR Green Master Mix (01000439, Thermo Fisher Scientific) were used for quantitative real-time PCR. The calculated cycle threshold values were normalized to the internal reference *GAPDH* level. Finally, each target gene's relative mRNA expression levels were determined as $2^{-\Delta\Delta Ct}$ values. Tsingke provided the primers, and the sequences are listed in Table 1.

2.7. Western blot assay

T24 and EJ-1 cells in good growth condition were inoculated in a sterile, 6-cm dish, and 350 or 250 μmol/L ILL were added to the high and low concentration groups, respectively. After continued culture for 48 hours, the cells were well mixed with 100 μL of radio immunoprecipitation assay lysis buffer and incubated on ice for 30 minutes to lyse the cells. The total protein in the cell supernatant was extracted, and the protein concentration was quantified using a BCA Protein Assay kit (PC0020, Solarbio). Aliquots (40 μg) of each protein sample were separated using sodium dodecyl sulfate-polyacrylamide gel electrophoresis and transferred onto a PVDF membrane (Millipore, Billerica, MA, USA). After blocking in PBS containing 5% nonfat dried milk and 0.05% Tween-20 for 1 hour, primary antibodies against B-cell lymphoma 2 (BCL-2), BCL-2 antagonist/killer 1 (BAK1), BCL-2–associated X protein (BAX), or Cytochrome C (CYCS) (1:1000, Cell Signaling Technology, USA) were incubated at 4°C overnight, and a monoclonal antibody against human β-actin (1:500; Cell Signaling Technology, USA) was used as an internal control. Finally, the bands were visualized using a Bio-Rad imaging system after incubation with a secondary antibody, and the images obtained were analyzed using the ImageJ software. This experiment was performed in triplicate.

2.8. Tumor growth in mice

5- to 6-week-old BALB/c female nude mice of specific pathogen-free grade (approximately 16 g) were used, purchased from SiPeifu Biotechnology Co. Ltd. (Beijing, China). Cells (5×10^6 cells/200 μL) were injected into the flank of each nude mouse. When the tumor volume reached approximately 60 mm^3, all the mice were randomly divided into 3 groups ($n = 5$). The low-dose group was injected intraperitoneally with 10 mg/kg ILL every 3 days, the high-dose group was injected intraperitoneally with 20 mg/kg ILL, and the control group was injected intraperitoneally with the same volume of PBS. All experimental mice (5 mice per cage) were housed under SPF conditions, with free access to irradiated sterilized experimental mouse maintenance feed (Jiangsu Synergy Pharmaceutical and Bioengineering Co., Ltd., Jiangsu, China) and water. In the barrier system, the room temperature was 20°–26°C, relative humidity was 40%–70%, air change was ≥15 times/hour, and light and dark alternated for 12 hours each day and night. Tumor volume (mm^3) was determined using the formula $a \times b^2 \times \pi/6$, where a is the longer diameter of the tumor and b is the shorter diameter. The tumor inhibition rate was $(A\text{-}B)/A \times 100\%$, where A is the average growth volume of the control group and B is the average growth volume of the experimental group. The experiment was terminated when the average tumor volume in the control group reached 1600 mm^3, and the subcutaneously implanted tumors were dissected, weighed, and preserved in 4% paraformaldehyde.

Table 1

Primers for RT-quantitative PCR.

Gene	Forward primer sequence (5′-3′)	Reverse primer sequence (5′-3′)
CASP10	TAGGATTGGTCCCCAACAAGA	GAGAAACCCTTTGTCGGGTGG
CYCS	GGTGATGTTGAGAAAGGCAAG	GTTCTTATTGGCGGCTGTGT
BAX	CCTTTTGCTTCAGGGTTTCA	CAGTTGAAGTTGCCGTCAGA
BCL-2	GGAGGATTGTGGCCTTCTTT	GCCGTACAGTTCCACAAAGG
NFκB1	ACTGTGAGGATGGGATCTGC	CCTTCTGCTTGCAAATAGGC
CASP8	TTTGACCACGACCTTTGAAGAG	CCCCTGACAAGCCTGAATAAAA
BAK1	TCTGGCCCTACACGTCTACC	ACAAACTGGCCCAACAGAAC
GAPDH	GGAGCGAGATCCCTCCAAAAT	GGCTGTTGTCATACTTCTCATGG

2.9. Hematoxylin-eosin staining and immunohistochemistry

Extracted tumor tissues were soaked in 4% paraformaldehyde for 48 hours and embedded in paraffin. The paraffin sections were baked at 60°C for 1 hour, deparaffinized, and rehydrated (100% xylene twice for 10 minutes each, 100% anhydrous ethanol for 10 minutes, 95% ethanol for 10 minutes, 75% ethanol for 10 minutes, and PBS for 10 minutes) before being used for hematoxylin-eosin staining and immunohistochemistry experiments. Hematoxylin-eosin staining using hematoxylin (2–6 minutes) and eosin (2–5 seconds) reagents were used to determine whether ILL destroyed the structure of the tumor tissue. The deparaffinized, hydrated tissues were subjected to microwave antigen repair with 0.01 mol/L citrate buffer and blocked with 5% bovine serum albumin for 20 minutes at room temperature. Then, primary antibodies (CYCS [1:100], BCL-2 [1:100], BAK1 [1:400], BAX [1:100]) were added and incubated at 4°C overnight. After blocking endogenous peroxidases with 3% hydrogen peroxide for 10 minutes at room temperature, the slides were incubated with secondary antibodies for 30–45 minutes. Color was developed at room temperature using a 3,3′-diaminobenzidine chromogenic agent, and the reaction time for all slides was 3 minutes. After counterstaining with hematoxylin for 15 seconds, the slides were dehydrated in ethanol, cleared in xylene, and sealed.

2.10. Statistical analysis

All statistical analyses were performed using the GraphPad Prism (version 8) software. Statistical data were tested for differences between groups using unpaired t tests and presented as the standard deviation of the mean ($n \geq 3$ independent repeated experiments, $n = 3$ multiple wells). $p < 0.05$ was considered statistically significant.

3. Results

3.1. ILL inhibited the viability of the T24 and EJ-1 BC cell lines

First, we investigated the cytotoxicity of ILL on various BC cell lines using the CCK-8 assay. The normal urothelial cell line SV-HUC-1 and BC cell lines, T24 and EJ-1, were treated with different concentrations of ILL (0, 10, 20, 50, 100, 200, 400, 600, 800, or 1000 μmol/L). The 24-hour IC_{50} values of ILL on SV-HUC-1, T24, and EJ-1 cell lines were 912.9 ± 1.32 μmol/L, 542.4 ± 2.176 μmol/L, and 568.7 ± 2.32 μmol/L, respectively. The 48-hour IC_{50} values were 931.8 ± 1.603, 301.7 ± 2.734, and 325.8 ± 2.598 μmol/L ($p < 0.05$) for SV-HUC-1, T24, and EJ-1 cell lines, respectively. With increasing time and concentration, the killing effect of ILL on BC cells increased; however, at the same concentrations, the killing effect on normal urothelial cells was significantly reduced (Fig. 2A, B). Thus, ILL can significantly inhibit the growth of BC cells without greater damage to the normal urinary tract epithelium, which is important in controlling the progression of BC. To achieve improved experimental effects, ILL administration at the concentrations of 250 or 350 μmol/L for 48 hours for T24 and EJ-1 cell lines was selected for subsequent experiments.

3.2. ILL reduced BC cell migration

We used wound healing assays to determine the effect of ILL on BC cell migration. Migration is one of the characteristic malignant

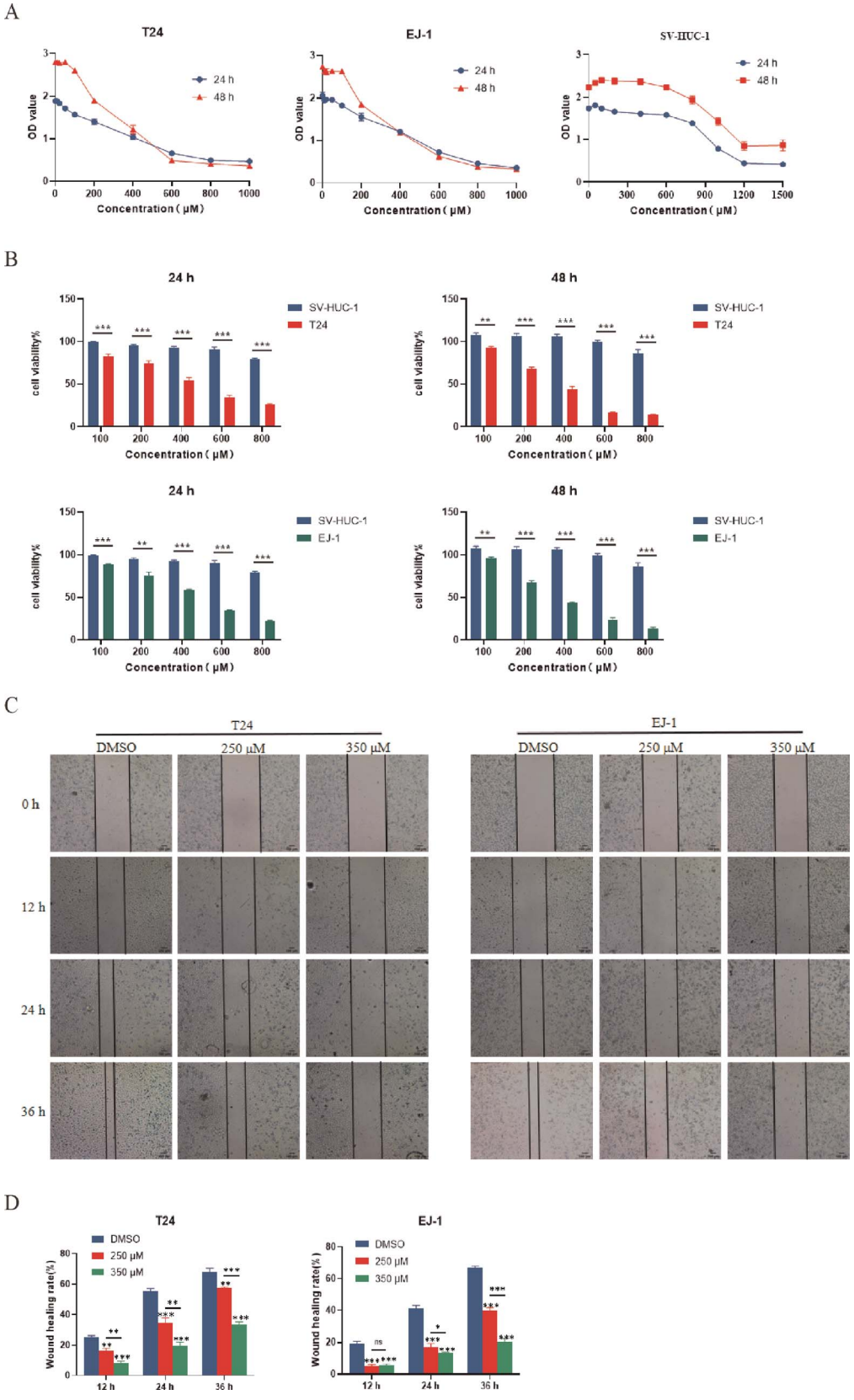

Figure 2. ILL inhibits the proliferation and migration of BC cell lines. (A) SV-HUC-1, T24, and EJ-1 cells were treated with different concentrations of ILL for 24 or 48 hours, and cell viability was detected by CCK-8 assay. (B) Cell viability of SV-HUC-1, BIU-87, or EJ-1 cells cocultured with ILL for 24 or 48 h. (C) Wound healing assay of T24 and EJ-1 cells treated with ILL. (D) Analysis of the migratory ability of T24 and EJ-1 BC cells before and after ILL treatment. Values are expressed as the mean ± SD of three independent experiments; $^{*}p < 0.05$, $^{**}p < 0.01$, $^{***}p < 0.001$. The IC_{50} values of the three cell lines at two time points (24 and 48 hour) were calculated using GraphPad Prism statistical software (version 8.0). BC = bladder cancer; IC_{50} = half-maximal inhibitory concentration; ILL = isolinderalactone.

behaviors of tumor cells and is the focus of tumor treatment. Reducing the migratory ability of tumor cells can greatly reduce the risk of distant metastasis in patients. The BC cell lines T24 and EJ-1 were treated with ILL at the concentrations of 250 or 350 μmol/L. The wound healing rates of BC cells at 12, 24, and 36 hours were 16.32% (p = 0.002), 34.79% (p < 0.001), and 57.44% (p = 0.004), respectively, for T24 cells, and 5.25% (p < 0.001), 17.03% (p < 0.001), and 40.04% (p < 0.001), respectively, for EJ-1 cells after treatment with 250 μmol/L ILL, which were lower than the closure rates 25.06%, 55.65%, and 67.67%, respectively, in the T24 DMSO, and 19.57%, 41.16%, and 67.00%, respectively, for EJ-1 DMSO control groups. After 350 μmol/L ILL treatment, the wound healing rates of BC cells at 12, 24, and 36 hours were 8.35% (p < 0.001), 19.55% (p < 0.001), and 33.84% (p < 0.001), respectively, for T24 cells, and 5.45% (p < 0.001), 13.33% (p < 0.001), and 20.26% (p < 0.001), respectively, for EJ-1 cells, which were also all lower than the control group (Fig. 2C, D). Our data show that ILL can inhibit not only the growth of BC cells but also their migration with time and concentration dependences, indicating that ILL may be a new drug for the clinical treatment of BC.

3.3. ILL blocks the BC cell cycle

Next, we analyzed the effect of ILL on the cell cycle distribution of BC cells by flow cytometry. Abnormal proliferation of tumor cells requires synthesizing a large amount of DNA to prepare for cell division. Therefore, the binding of propidium iodide to nucleic acid bases can be used to detect the relationship between DNA quantity and cell cycle changes using flow cytometry. Bladder cancer cell lines T24 and EJ-1 were treated with ILL at 2 concentrations of 250 and 350 μmol/L for 48 hours, followed by cell cycle analysis. Isolinderalactone induced G0/G1 phase arrest in T24 and EJ-1 cells in a concentration-dependent manner and decreased the percentage of S phase cells, but no difference was observed in the percentage of cells in the G2/M phase (Fig. 3A). The percentage of G0/G1 phase cells in the T24 and EJ-1 DMSO control groups were 34.36% and 47.19%, respectively. After ILL treatment of 250 and 350 μmol/L, the percentage of G0/G1 phase cells increased to 46.42% (p = 0.016) and 64.62% (p < 0.001), respectively, for T24 cells, and 65.10% (p < 0.001) and 75.44% (p < 0.001), respectively, for EJ-1 cells (Fig. 3B). These results indicate that cell cycle arrest in the G0/G1 phase of BC cells treated with ILL could inhibit the proliferation of BC cells by blocking DNA synthesis.

3.4. ILL promotes BC cell apoptosis and its molecular mechanism

Flow cytometry and annexin V-FITC/PI double staining were used to observe the effect of ILL on BC cell apoptosis. Isolinderalactone promoted apoptosis of T24 and EJ-1 cells in a concentration-dependent manner. The percentage of apoptotic cells were 7.40% (p < 0.001) and 11.23% (p = 0.001) in T24 cells, and 12.60% (p = 0.003) and 25.69% (p < 0.001) in EJ-1 cells at ILL concentrations of 250 and 350 μmol/L, respectively, which were significantly higher than those of the DMSO-treated control groups, 1.88% and 3.00% for T24 cells, and 5.23% and 5.92% for EJ-1 cells (Fig. 4A, B).

Isolinderalactone can effectively arrest the cell cycle, inhibit cell viability, and promote apoptosis in BC cells. In addition, phytochemotherapeutic drugs induce endogenous apoptosis mainly through cytotoxic effects, with mitochondria playing an important role in this process. Therefore, to further clarify whether ILL induces BC apoptosis through mitochondria-mediated endogenous pathways, we used quantitative real-time PCR and western blot to investigate the molecular mechanisms of action of ILL at the gene and protein levels. The quantitative real-time PCR results showed that the expressions of mitochondria-related proapoptotic genes, *CASP10* (p = 0.002 and p < 0.001), *CYCS* (p < 0.001 and p = 0.026), *BAX* (p = 0.043 and p = 0.001), and *BAK1* (p = 0.025 and p = 0.013), were detected in T24 and EJ-1 cell lines treated with 300 μmol/L ILL and were significantly upregulated compared with those in the control group. However, the antiapoptotic gene *BCL-2* (p = 0.003, p < 0.001) was upregulated in both cell lines, and the proapoptotic gene *CASP8* (p < 0.001) was downregulated in T24 cells, contrary to expectations. In addition, the proliferation-regulated gene *BID* (p = 0.011) and the epithelial-mesenchymal transition-associated gene *NFκB1* (p = 0.017) were downregulated only in T24 cells. The tumor suppressor gene *TP53* was not significantly changed in either cell line (p = 0.537, p = 0.073) (Fig. 4C, D). In addition, we also verified gene expression using western blot. After treating T24 and EJ-1 cell lines with 250 or 350 μmol/L ILL for 48 h, compared with those in the control group, the proapoptotic proteins BAX (p = 0.001 and p < 0.001 for T24, and p = 0.002 and p < 0.001 for EJ-1), BAK1

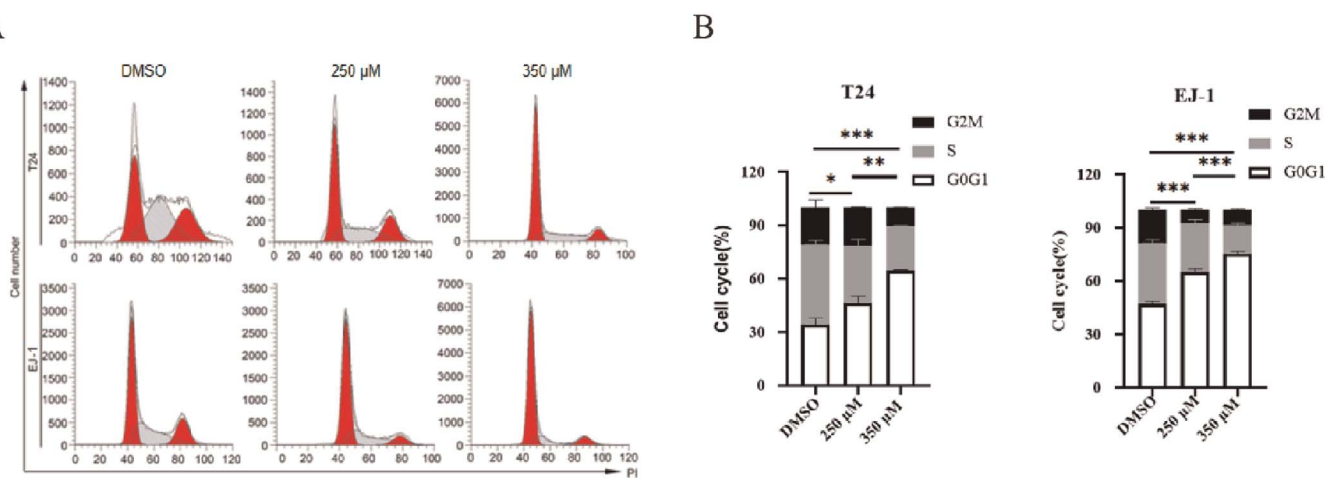

Figure 3. Effect of ILL on the BC cell cycle. (A–B) BC cell lines T24 and EJ-1 were treated with 250 or 350 μmol/L ILL or DMSO for 48 h, and the cell cycle was analyzed by PI staining and flow cytometry. *p < 0.05, **p < 0.01, ***p < 0.001. BC = bladder cancer; DMSO = dimethyl sulfoxide; ILL = isolinderalactone; PI = propidium iodide.

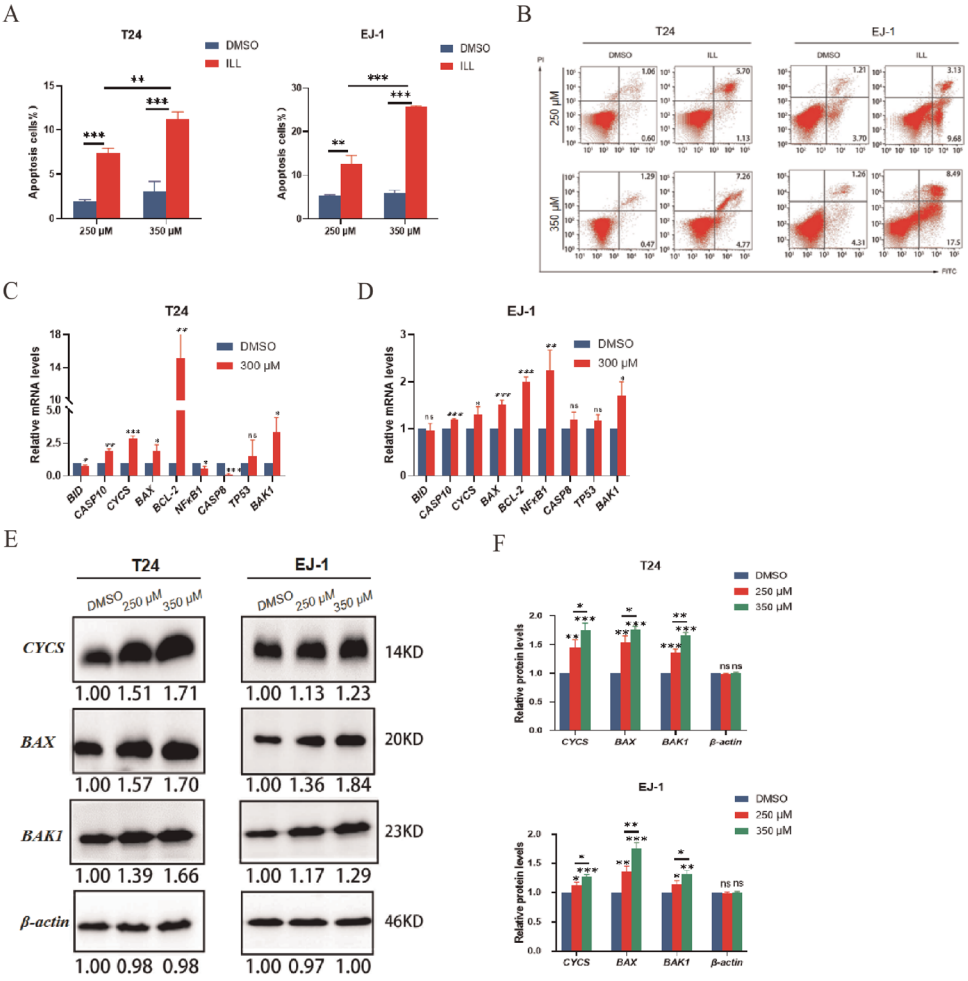

Figure 4. Effect of ILL on apoptosis in BC cells. (A) BC cell lines T24 and EJ-1 were treated with 250 or 350 μmol/L ILL or DMSO as a control for 48 hours. (B) Apoptosis was analyzed via Annexin V-FITC/PI double staining and flow cytometry. (C–D) mRNA levels of apoptosis-related genes in T24 and EJ-1 cell lines after ILL treatment were analyzed using RT-PCR, with *GAPDH* as an internal control. (E–F) WB analysis of apoptosis-related proteins. β-Actin was used as a loading control. Data are presented as mean ± SD. $p > 0.05$ (not significant), $^{*}p < 0.05$, $^{**}p < 0.01$, $^{***}p < 0.001$. BC = bladder cancer; DMSO = dimethyl sulfoxide; FITC = fluorescein isothiocyanate; ILL = isolinderalactone; PI = propidium iodide; WB = western blot.

($p = 0.001$ and $p < 0.001$ for T24, and $p = 0.012$ and $p = 0.001$ for EJ-1), and CYCS ($p = 0.004$ and $p < 0.001$ for T24, and $p = 0.011$ and $p < 0.001$ for EJ-1) were significantly elevated, and the upregulation of the target proteins significantly increased with increasing ILL concentration, whereas there was no significant difference in reference β-actin ($p = 0.158$ and $p = 0.374$ for T24, and $p = 0.329$ and $p > 0.999$ for EJ-1) (Fig. 4E, F). Therefore, ILL can promote BC cell apoptosis by regulating mitochondria-related apoptosis genes, thereby inhibiting the progression of BC.

3.5. Antitumor effect of ILL in vivo

To evaluate the inhibitory effect of ILL on bladder tumor growth in vivo, the inhibitory effect of ILL on bladder tumor growth in vivo was observed by establishing a subcutaneous implantation tumor model in mice with intraperitoneal administration of ILL (Fig. 5A). The pathological changes in the tumor tissues before and after drug treatment were observed using Hematoxylin-eosin staining. The expression of apoptosis-related proteins before and after pharmacological therapy was examined using immunohistochemistry.

Isolinderalactone treatment drastically decreased xenograft growth rates in mice bearing T24 or EJ-1 BC tumors. After 1 week of low-dose (10 mg/kg) or high-dose (20 mg/kg) ILL treatment, the tumor volumes of T24 ($p < 0.001$ and $p < 0.001$, respectively) or EJ-1 ($p < 0.001$ and $p < 0.001$, respectively) tumor-bearing mice were significantly reduced compared with the control groups. After 25 days of ILL administration, the tumor inhibition rates of in the high-dose group were 75.24% for T24 and 71.58% for EJ-1, while the tumor inhibition rates in the low-dose group were 47.43% for T24 and 43.89% for EJ-1, and the tumor mass also decreased with an increase in drug concentration (Fig. 5B–G).

Hematoxylin-eosin staining revealed that ILL destroyed the structure of tumor tissue. With an increase in drug concentration, the destructive power of ILL on tumor cells and cell stroma was enhanced, connective tissue and angiogenesis in tumor tissue were significantly reduced, integrity of cells was destroyed, and chromatin was deposited (Fig. 5H). Importantly, semiquantitative analysis revealed that the proapoptotic proteins CYCS ($p < 0.001$, $p < 0.001$), BAX ($p = 0.001$, $p = 0.001$), and BAK1 ($p = 0.001$, $p < 0.001$) were significantly upregulated in T24 and EJ-1 xenografts after treatment with 20 mg/kg ILL. The target proteins were diffusely distributed at the damaged sites in the tumor tissue (Fig. 5I, J). In conclusion, ILL inhibits the growth of bladder tumors

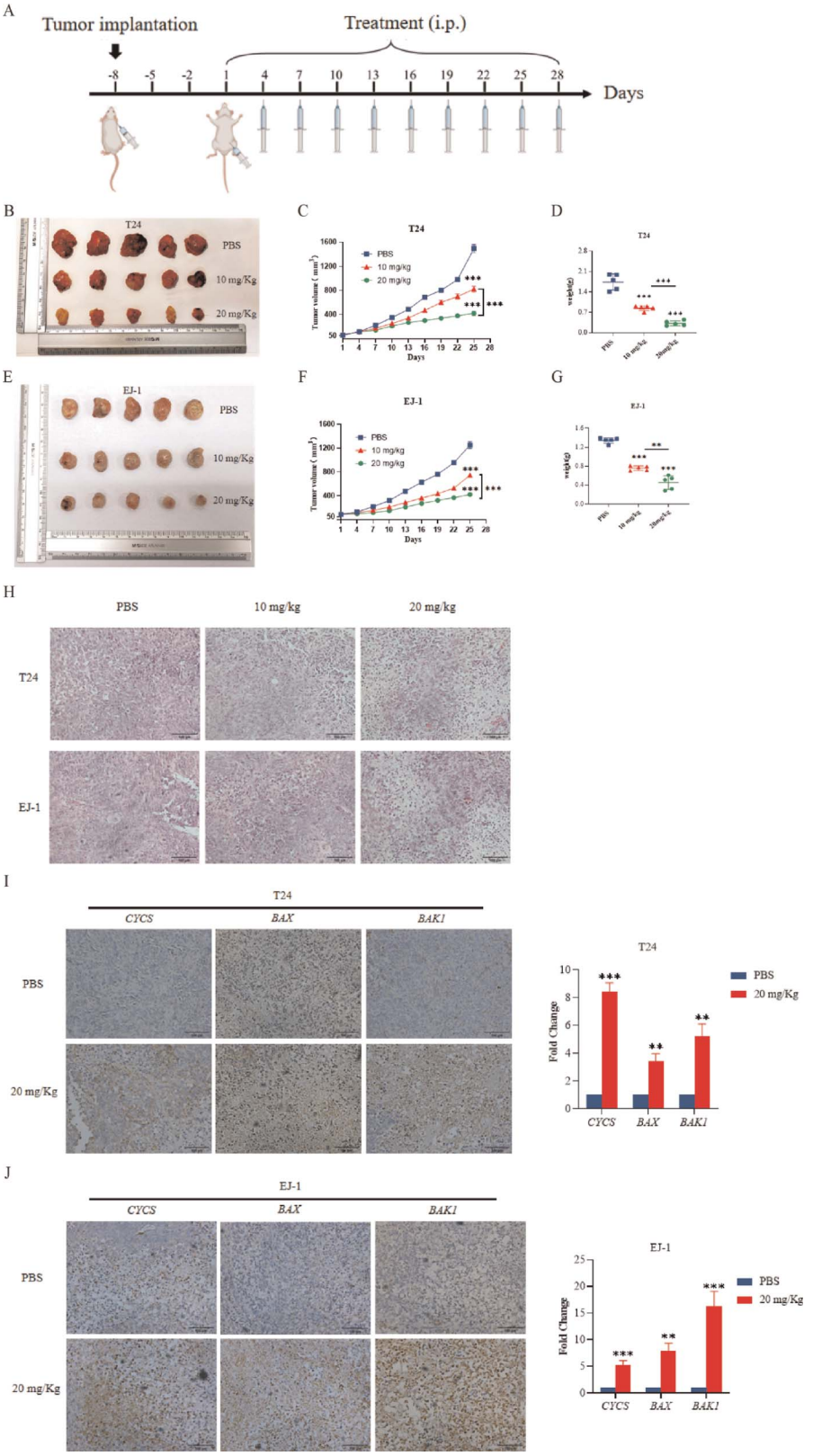

Figure 5. ILL limits tumor growth in murine BC xenografts in vivo. (A) Timeline of tumor formation and administration in the mouse BC xenograft model. (B) BC T24 cell xenograft tumors before and after ILL treatment. (C–D) Changes in tumor volume and weight after intraperitoneal injection of ILL at different concentrations or DMSO as a control. (E) EJ-1 BC xenograft tumors before and after ILL treatment. (F–G) EJ-1 BC xenograft tumor volume and weight changes following intraperitoneal injection of ILL at various doses or DMSO as a control. (H) HE staining of subcutaneously implanted BC tumors in nude mice treated with ILL at different concentrations. (I–J) IHC staining and semiquantitative analysis of target proteins in bladder T24 and EJ-1 cell lines before and after ILL treatment (original magnification, 200×). Values are expressed as the standard deviation of the mean; $^{**}p < 0.01$, $^{***}p < 0.001$. BC = bladder cancer; DMSO = dimethyl sulfoxide; HE = hematoxylin-eosin; IHC = immunohistochemistry; ILL = isolinderalactone.

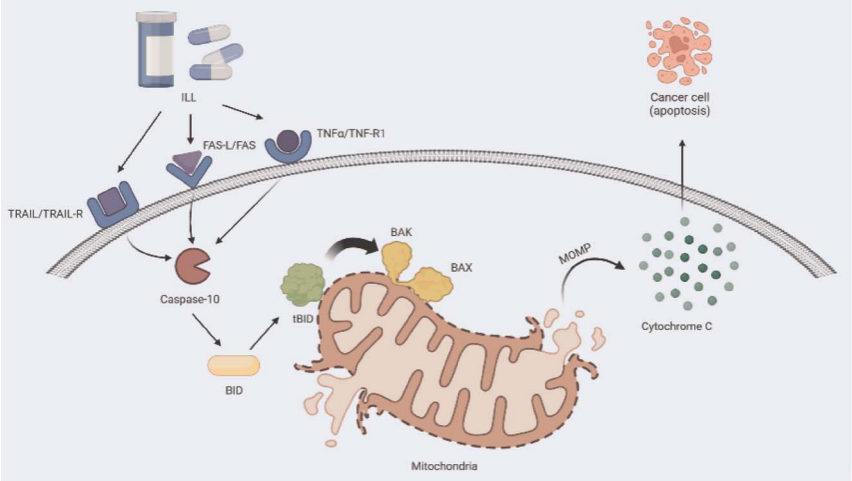

Figure 6. Mechanism of ILL-induced apoptosis in T24 and EJ-1 cells. BAK = BCL-2-antagonist/killer 1; BAX = BCL-2-associated X; BID = BH3-interacting domain death agonist; FAS = Fas cell surface death receptor; FAS-L = Fas ligand; ILL = isolinderalactone; MOMP = mitochondrial outer membrane permeabilisation; TRAIL = TNF-related apoptosis-inducing ligand; TRAIL-R = TNF-related apoptosis-inducing ligand receptor; TNFα = tumour necrosis factor-α; TNF-R1 = tumour necrosis factor receptor 1; tBID = truncated BID.

in vivo and promotes the destruction of the tumor structure by modulating the expression of apoptotic target proteins.

In summary, our results suggest that ILL inhibits the proliferation of BC cells by blocking the cell cycle and inducing apoptosis. Further studies of the molecular mechanism showed that ILL can promote apoptosis by regulating the expression of proapoptotic proteins BAK1, BAX, and CYCS as well as the antiapoptotic protein BCL-2. In addition, in vivo, ILL showed excellent antitumor growth effects (Fig. 6).

4. Discussion

Bladder cancer is the most common malignant tumor of the urinary system. Methods for early BC diagnosis are improving,[15] and its pathogenesis and treatment have been widely studied. The treatment of patients with advanced BC has undergone rapid changes. Checkpoint inhibitors, targeted therapy, and antibody-drug conjugate immunotherapy are options for patients at different disease stages.[16] This has led to great progress in the survival rates of patients with BC. However, owing to the high recurrence rate of NMIBC and high mortality rate of advanced MIBC, and the heterogeneity, drug resistance, and strong toxic side effects of tumors, safer and more effective drug development and mechanism of action research are particularly important.

In this study, ILL inhibited the proliferation of BC cells in vitro by stopping the BC cell cycle in the G0/G1 phase, and also significantly reduced BC migration and induced apoptosis in BC cells. In addition, we established a BALB/C tumor-bearing mouse model to determine the antitumor effect of ILL in vivo, and found that ILL can effectively inhibit tumor growth. Isolinderalactone treatment decreased tumor volume and very low toxicity with increasing drug concentration. Therefore, our study is the first to show that ILL can significantly inhibit the development of BC both in vivo and in vitro. Isolinderalactone exerts antitumor effects by inhibiting tumor angiogenesis.[17] Although there is a lack of knowledge regarding the mechanisms and safety of herbal extract compounds and derivatives in clinical cancer therapy, they are gradually becoming candidates for antitumor drugs because of their easy availability and few side effects.[18,19] For example, taxol, isolated from Taxus chinensis, is a common clinical antitumor drug with a definite effect on the treatment of BC.[20,21] Flavonoids and the Mediterranean diet also demonstrate protective action in reducing the risk of BC.[22] Therefore, the new discovery of ILL's effects on BC may offer novel evidence for the treatment of BC, thereby potentially benefiting patients with BC clinically.

In addition, ILL upregulates mitochondrial superoxide, downregulates mitochondrial superoxide dismutase 2, and inactivates the signal transducer and activator of transcription 3-mediated pathway to induce ovarian cancer cell death.[23] Furthermore, ILL reduces the antiapoptotic X-linked inhibitor of apoptosis protein and BCL-2 proteins, thereby increasing caspase-3 lysis and apoptosis, and retarding tumor growth in human glioblastomas in vitro and in vivo.[14] Isolinderalactone also induces apoptosis in human non–small cell lung cancer and colorectal cancer.[24,25] Overall, ILL has certain advantages in antitumor treatment.

Furthermore, we explored the potential mechanism by which ILL inhibits BC progression. We found that ILL promotes BC cell apoptosis by regulating the BCL-2 family and CYCS, thereby inhibiting BC cell growth. Isolinderalactone induced the apoptosis of BC cells through the endogenous pathway. However, we found that the *BCL-2* gene was not inhibited, suggesting that ILL may regulate *BAX* and *BAK1* expression through the Caspase-8/10 pathway, thereby promoting mitochondria-related apoptosis. Apoptosis can be activated either by an extrinsic pathway initiated by death receptors or by an intrinsic pathway through mitochondria to prevent tumor formation. The intrinsic pathway of apoptosis requires the activation of cytosolic caspases through the release of mitochondrial cytochrome C, and involves permeabilization of the mitochondrial outer membrane controlled by the BCL-2 family of proteins.[26–29] The BCL-2 protein family is divided into the following 3 categories based on their major functions: antiapoptotic proteins (BCL-2, BCL-XL, BCL-W, MCL-1, and BFL-1/A1), proapoptotic proteins (BAX, BAK1, and BOK), and proapoptotic BH3-only proteins (BAD, BID, BIK, BIM, BMF, HRK, NOXA, and PUMA).[30–32] The Caspase family comprises cysteine proteases with Caspase-8 and Caspase-10 playing a very important role in the regulation of cell apoptosis. Tumor necrosis factor–related apoptosis-inducing ligand and tumor necrosis factor-α and FAS ligand can activate Caspase-8 and

Caspase-10 upon binding to their receptors. Activated Caspase-8/10 cleaves cytosolic BH3 interacting-domain death agonist (BID) to form a potent tBID protein. The transfer of tBID to the mitochondrial membrane enriches BAX and BAK1 in the cytoplasm and downregulates BCL-2 expression, resulting in a change in mitochondrial membrane permeability, promotion of CYCS in the cytoplasm, and induction of apoptosis in BC cells. Intravesical immunotherapy with a BCG vaccine is the standard treatment for high-risk NMIBC.[33] Bladder cancer cells treated with BCG also induce the activation of Caspase-8 and Caspase-10 through factor–related apoptosis-inducing ligand activation, thereby inducing apoptosis in BC cells.[34] In the present study, we also confirmed that Caspase-10 was upregulated in BC cells after treatment with ILL, providing a new idea for the combined treatment with ILL and BCG vaccines for BC. However, in this study, the causal relationship of the molecular mechanisms has not been studied comprehensively, and the specific regulatory mechanism needs to be confirmed by further studies. The existence of other ways for ILL to exert its antitumor effects also needs to be studied. In addition, the study requires further follow-up clinical studies to explore better dosing regimens.

The past decade has witnessed a rapid surge in the availability of therapeutic choices for BC because of an improved comprehension of its pathogenesis and an increasing focus on clinical drug development for BC.[35] Currently, Chinese herbal extracts are getting increasing attention and are being used more often in the clinic, but there is still a big gap in the mechanism of action of chemotherapeutic drugs. Several studies have described the cytotoxicity of chemotherapeutic drugs inducing apoptosis in tumor cells. In this study, we confirmed that ILL alters mitochondrial function and induces apoptosis by regulating the expression of BCL family proteins. This undoubtedly provides a new direction for the clinical treatment of BC. An in-depth investigation into the efficacy of ILL and whether its combination with other commonly used antitumor drugs is needed can lead to a better prognosis for patients with BC and help clinicians combat BC more effectively.

5. Conclusions

We demonstrated, for the first time, that ILL exerts antitumor activity in BC in vitro by inhibiting cell proliferation and migration and inducing cell cycle arrest in the G0/G1 phase. Further analysis highlighted that ILL modulated the expression of the BCL-2 protein family to alter the membrane permeability of mitochondria and increased the release of cytochrome C, thereby inhibiting the proliferation, invasion, migration, and apoptosis of BC cells and significantly reducing tumor growth in vivo. Based on these results, ILL may be a potential therapeutic strategy for BC.

Acknowledgments

None.

Statement of ethics

All the experimental protocols for animal studies were conducted in accordance with the National Institutes of Health Guide for the Care and Use of Laboratory Animals. This study was approved by the laboratory animal welfare ethics committee of Yunnan University (Approval No. YNU20230653).

Conflict of interest statement

The authors declare no conflicts of interest.

Funding source

This work was supported by the Fundamental Research Funds for the Central Universities (No. buctrc201910), Young Elite Scientists Sponsorship Program by Xinjiang Association for Science and Technology (2021), basic research program of Yunnan Science and Technology Department and Kunming Medical University (202101AY070001-144), and the scientific research project of Education Department of Yunnan Province (No. 2024Y231).

Author contributions

HW, ZY: Conceived and designed the experiments;
QW, WX: Performed the experiments;
LY: Conducted the animal study;
HS, YS, WF, HX, JX, HW: Analyzed the data;
QW: Drafted the manuscript;
HW, ZY, WX, LY, HS, YS, WF, HX, JX, HW: Revised the manuscript.

Data availability

The datasets generated during and/or analyzed during the current study are not publicly available, but are available from the corresponding author on reasonable request.

References

[1] Sung H, Ferlay J, Siegel RL, et al. Global cancer statistics 2020: GLOBOCAN estimates of incidence and mortality worldwide for 36 cancers in 185 countries. *CA Cancer J Clin* 2021;71(3):209–249.
[2] van den Bosch S, Alfred Witjes J. Long-term cancer-specific survival in patients with high-risk, non-muscle-invasive bladder cancer and tumour progression: A systematic review. *Eur Urol* 2011;60(3):493–500.
[3] Chamie K, Litwin MS, Bassett JC, et al. Recurrence of high-risk bladder cancer: A population-based analysis. *Cancer* 2013;119(17):3219–3227.
[4] Milowsky MI, Rumble RB, Booth CM, et al. Guideline on muscle-invasive and metastatic bladder cancer (European Association of Urology Guideline): American Society of Clinical Oncology Clinical Practice Guideline Endorsement. *J Clin Oncol* 2016;34(16):1945–1952.
[5] Shi ZD, Hao L, Han XX, et al. Targeting HNRNPU to overcome cisplatin resistance in bladder cancer. *Mol Cancer* 2022;21(1):37.
[6] Leung EL-H, Fan X-X, Wong MP, et al. Targeting tyrosine kinase inhibitor-resistant non-small cell lung cancer by inducing epidermal growth factor receptor degradation via methionine 790 oxidation. *Antioxid Redox Signal* 2016;24(5):263–279.
[7] Li RZ, Fan XX, Duan FG, et al. Proscillaridin A induces apoptosis and suppresses non-small-cell lung cancer tumor growth via calcium-induced DR4 upregulation. *Cell Death Dis* 2018;9(6):696.
[8] Han C, Wang Z, Chen S, et al. Berbamine suppresses the progression of bladder cancer by modulating the ROS/NF-κB Axis. *Oxid Med Cell Longev* 2021;2021:8851763.
[9] Gong H, Chen W, Mi L, et al. Qici Sanling decoction suppresses bladder cancer growth by inhibiting the Wnt/B-catenin pathway. *Pharm Biol* 2019;57(1):507–513.
[10] Banik K, Khatoon E, Harsha C, et al. Wogonin and its analogs for the prevention and treatment of cancer: A systematic review. *Phytother Res* 2022;36(5):1854–1883.
[11] Chuang C-H, Wang L-Y, Wong YM, Lin E-S. Anti-metastatic effects of isolinderalactone via the inhibition of MMP-2 and up regulation of NM23-H1 expression in human lung cancer A549 cells. *Oncol Lett* 2018;15(4):4690–4696.
[12] Yen MC, Shih YC, Hsu YL, et al. Isolinderalactone enhances the inhibition of SOCS3 on STAT3 activity by decreasing miR-30c in breast cancer. *Oncol Rep* 2016;35(3):1356–1364.
[13] Lee SY, Park JH, Cho KH, Kim H, Shin HK. Isolinderalactone inhibits glioblastoma cell supernatant-induced angiogenesis. *Oncol Lett* 2022;24(4):328.
[14] Hwang JY, Park JH, Kim MJ, et al. Isolinderalactone regulates the BCL-2/caspase-3/PARP pathway and suppresses tumor growth in a human glioblastoma multiforme xenograft mouse model. *Cancer Lett* 2019;443:25–33.

[15] Calace FP, Napolitano L, Arcaniolo D, et al. Micro-ultrasound in the diagnosis and staging of prostate and bladder cancer: A comprehensive review. *Medicina (Kaunas)* 2022;58(11):1624.
[16] Lenis AT, Lec PM, Chamie K, Mshs MD. Bladder cancer: A review. *JAMA* 2020;324(19):1980–1991.
[17] Park JH, Kim MJ, Kim WJ, et al. Isolinderalactone suppresses human glioblastoma growth and angiogenic activity in 3D microfluidic chip and in vivo mouse models. *Cancer Lett* 2020;478:71–81.
[18] Ding X, Zhu FS, Li M, Gao SG. Induction of apoptosis in human hepatoma SMMC-7721 cells by solamargine from Solanum nigrum L. *J Ethnopharmacol* 2012;139(2):599–604.
[19] Meng Z, Li T, Ma X, et al. Berbamine inhibits the growth of liver cancer cells and cancer-initiating cells by targeting Ca^{2+}/calmodulin-dependent protein kinase II. *Mol Cancer Ther* 2013;12(10):2067–2077.
[20] Michaelson MD, Hu C, Pham HT, et al. A phase 1/2 trial of a combination of paclitaxel and trastuzumab with daily irradiation or paclitaxel alone with daily irradiation after transurethral surgery for noncystectomy candidates with muscle-invasive bladder cancer (trial NRG oncology RTOG 0524). *Int J Radiat Oncol Biol Phys* 2017;97(5):995–1001.
[21] Robins DJ, Sui W, Matulay JT, et al. Long-term survival outcomes with intravesical nanoparticle albumin-bound paclitaxel for recurrent non-muscle-invasive bladder cancer after previous Bacillus Calmette-Guérin therapy. *Urology* 2017;103:149–153.
[22] Aveta A, Cacciapuoti C, Barone B, et al. The impact of meat intake on bladder cancer incidence: Is it really a relevant risk? *Cancers (Basel)* 2022;14(19):4775.
[23] Rajina S, Kim WJ, Shim JH, et al. Isolinderalactone induces cell death via mitochondrial superoxide- and STAT3-mediated pathways in human ovarian cancer cells. *Int J Mol Sci* 2020;21(20):7530.
[24] Chang WA, Lin ES, Tsai MJ, Huang MS, Kuo PL. Isolinderalactone inhibits proliferation of A549 human non-small cell lung cancer cells by arresting the cell cycle at the G0/G1 phase and inducing a Fas receptor and soluble Fas ligand-mediated apoptotic pathway. *Mol Med Rep* 2014;9(5):1653–1659.
[25] Kwak AW, Park JW, Lee SO, et al. Isolinderalactone sensitizes oxaliplatin-resistance colorectal cancer cells through JNK/p38 MAPK signaling pathways. *Phytomedicine* 2022;105:154383.
[26] Cory S, Huang DC, Adams JM. The Bcl-2 family: Roles in cell survival and oncogenesis. *Oncogene* 2003;22(53):8590–8607.
[27] Oltvai ZN, Milliman CL, Korsmeyer SJ. Bcl-2 heterodimerizes in vivo with a conserved homolog, Bax, that accelerates programmed cell death. *Cell* 1993;74(4):609–619.
[28] Hardwick JM, Soane L. Multiple functions of BCL-2 family proteins. *Cold Spring Harb Perspect Biol* 2013;5(2):a008722.
[29] Wang C, Youle RJ. The role of mitochondria in apoptosis*. *Annu Rev Genet* 2009;43:95–118.
[30] Kale J, Osterlund EJ, Andrews DW. BCL-2 family proteins: Changing partners in the dance towards death. *Cell Death Differ* 2018;25(1):65–80.
[31] Warren CFA, Wong-Brown MW, Bowden NA. BCL-2 family isoforms in apoptosis and cancer. *Cell Death Dis* 2019;10(3):177.
[32] Delbridge ARD, Grabow S, Strasser A, Vaux DL. Thirty years of BCL-2: Translating cell death discoveries into novel cancer therapies. *Nat Rev Cancer* 2016;16(2):99–109.
[33] Del Giudice F, Flammia RS, Chung BI, et al. Compared efficacy of adjuvant intravesical BCG-TICE vs. BCG-RIVM for high-risk non-muscle invasive bladder cancer (NMIBC): A propensity score matched analysis. *Cancers (Basel)* 2022;14(4):887.
[34] Han J, Gu X, Li Y, Wu Q. Mechanisms of BCG in the treatment of bladder cancer-Current understanding and the prospect. *Biomed Pharmacother* 2020;129:110393.
[35] Patel VG, Oh WK, Galsky MD. Treatment of muscle-invasive and advanced bladder cancer in 2020. *CA Cancer J Clin* 2020;70(5):404–423.

How to cite this article: Wang Q, Xu W, Ying L, Shi H, Sun Y, Feng W, Xu H, Xie J, Wei H, Yang Z, Wang H. Preliminary study of the mechanism of isolinderalactone inhibiting the malignant behavior of bladder cancer. *Curr Urol* 2025;19(1):49–58. doi: 10.1097/CU9.0000000000000259